NANOSYSTEMS:
PHYSICS, CHEMISTRY, MATHEMATICS

Pakholchuk P.P., et al. *Nanosystems: Phys. Chem. Math.*, 2025, **16** (6), 908–914.
http://nanojournal.ifmo.ru
DOI 10.17586/2220-8054-2025-16-6-908-914

Original article

Formation of laser-induced periodic surface structures on an $As_{50}Se_{50}$ film under femtosecond laser irradiation with wavelengths of 400–800 nm

Petr P. Pakholchuk[1,2,a], Dmitrii V. Shuleiko[2,b], Vadim A. Barbashov[1,c], Stanislav V. Zabotnov[2,d], Sergey A. Kozyukhin[3,e], Pavel K. Kashkarov[2,4,f]

[1]Lebedev Physical Institute, Russian Academy of Sciences, Moscow 119991, Russia

[2]Faculty of Physics, Moscow State University, Moscow 119991, Russia

[3]Kurnakov Institute of General and Inorganic Chemistry, Moscow 119071, Russia

[4]National Research Centre "Kurchatov Institute", Moscow 123182, Russia

[a]p.paholchuk@lebedev.ru, [b]shuleyko.dmitriy@physics.msu.ru, [c]barbashovva@lebedev.ru, [d]zabotnov@physics.msu.ru,[e]sergkoz@igic.ras.ru, [f]kashkarov@physics.msu.ru

Corresponding author: P. P. Pakholchuk, p.paholchuk@lebedev.ru

PACS 42.62.-b, 78.20.Fm, 78.67.-n

ABSTRACT Laser-induced periodic surface structures (LIPSS) on chalcogenide glassy semiconductors are of great interest in relation with creating polarization-sensitive optical elements. This study investigates the formation of LIPSS on the surface of $As_{50}Se_{50}$ amorphous film, fabricated by thermal vacuum deposition, under femtosecond laser irradiation in the wavelength range from 400 to 800 nm. The periods of various LIPSS types depend linearly on the laser wavelength. The measured birefringence of so-called low spatial frequency LIPSS, formed by different irradiation wavelengths, are in the 10–85 nm range. The maximum birefringence of 85 nm was obtained for structures irradiated at a 480 nm wavelength. A significant decrease in birefringence was observed at a wavelength of 800 nm, which may be due to the formation of a less pronounced and more disordered surface relief caused by less effective absorption of modifying laser radiation with photon energy lower than optical band gap of $As_{50}Se_{50}$. Decreased optical absorption observed in $As_{50}Se_{50}$ films with LIPSS is caused by increased light scattering on the surface relief.

KEYWORDS laser-induced periodic surface structures, $As_{50}Se_{50}$ amorphous films, laser-induced birefringence, optical retardance.

ACKNOWLEDGEMENTS This work was supported by the Russian Science Foundation (Grant No. 22-19-00035-II, https://rscf.ru/project/22-19-00035/

FOR CITATION Pakholchuk P.P., Shuleiko D.V., Barbashov V.A., Zabotnov S.V., Kozyukhin S.A., Kashkarov P.K. Formation of laser-induced periodic surface structures on an $As_{50}Se_{50}$ film under femtosecond laser irradiation with wavelengths of 400–800 nm. *Nanosystems: Phys. Chem. Math.*, 2025, **16** (6), 908–914.

1. Introduction

Chalcogenide glassy semiconductors (ChGS) of As-Se system are attracting attention due to their unique properties such as transparency in infrared region of the spectrum, high stability and a number of photoinduced phenomena (photodarkening, photobleaching, photocrystallization, etc.) [1–3]. Recently, high attention has been paid to the nonlinear optical properties of ChGS. Measurements of nonlinear refractive index have shown that its value can range from 100 to 1000 times of that in silica glass. A high nonlinear refractive index combined with moderate to low nonlinear absorption makes materials suitable for all-optical signal processing devices, enhancing the performance of telecommunication systems ChGS are very suitable for these kinds of applications, because they are compatible with well-established silica-on-silicon and fiber drawing technologies. Photoinduced phenomena allow the local modification of the material properties by the exposure to suitable radiation which can be utilized in writing waveguide channels, diffraction gratings and so forth [4–6]. The formation of laser-induced surface periodic structures (LIPSS) [7–9] on such materials is of particular interest in this case.

The formation of LIPSS is observed on a wide variety of materials – metals, semiconductors, and dielectrics, both crystalline and amorphous [10] – typically upon irradiation with ultrashort high-power laser pulses. This periodic relief demonstrates a clear relationship with the wavelength and polarization direction of the laser radiation used, and the process of its formation is mainly explained by the excitation of surface electromagnetic waves and their subsequent interference with the incident laser radiation [11, 12]. The main types of such relief include so-called low spatial frequency LIPSS (LSFL), characterized by the ridges orthogonal to the polarization and a period approximately equal to the laser radiation wavelength, and high spatial frequency LIPSS (HSFL) with ridges orientation along the polarization and a period several

times shorter than the wavelength [7, 13]. It has previously been shown that LIPSS formed on As-Se ChGS films can exhibit birefringence [14], which is explained by the form anisotropy of the relief. This allows for laser-structured ChGS films to be considered as a basis for creating optical polarizing elements. The parameters of the LIPSS formed on films are influenced by many factors. These include the film material and thickness, the substrate material, the laser pulses fluence and number, as well as the wavelength. Most studies investigate the dependence of LIPSS generation on various materials upon changing the fluence and number of laser pulses. At the same time, the laser wavelength used affects not only the LIPSS period, but can also significantly affect the depth of the formed relief [15, 16] and, accordingly, the optical anisotropy.

In the present study, our aim was forming LIPSS by exposing an $As_{50}Se_{50}$ amorphous thin film to femtosecond laser pulses of varying wavelengths (400–800 nm) in order to analyze birefringence and optical transmittance of the resulting structured surfaces. We note that during the experiments, the energy and number of laser pulses were also adjusted for different wavelengths to achieve sustainable and uniform LIPSS formation in each case.

2. Materials and methods

The $As_{50}Se_{50}$ bulk glass used in our experiments was obtained under the following conditions: the respective amounts of arsenic and selenium with 5N purity were placed in quartz ampoule evacuated down to $\sim 10^{-3}$ Pa and heated in a rotary furnace. The temperature was maintained constant at the glass melting point while the melt was continuously stirred to ensure better homogenization. After preservation at 900 K for several hours, the melt was cooled by air quenching. The glassy state of the obtained samples was controlled by the characteristic conchoidal fracture in glass. Then the film was produced from the respective bulk glassy sample by thermal evaporation process using a UVN-2M unit, at a temperature of 700–800 K and a residual pressure of less than 5 10^{-4} Pa. A molybdenum boat was used as a resistive evaporator; the distance between the substrate and the evaporator was 15.5 cm, the sample weight was 0.005 g and sublimation duration was 20 sec. The process of material deposition was controlled by visual observation. In order to avoid thickness non-uniformities, the substrate was rotated during the evaporation process. Following the completion of the deposition process, the substrate was left in a vacuum chamber until its complete cooling to room temperature. The fabricated $As_{50}Se_{50}$ film thickness, determined by atomic-force microscopy (AFM) was 840 ± 10 nm.

As a source of femtosecond laser radiation for the film surface structuring, a TETA-20 laser system (Avesta-Project Ltd, Russia; maximum power 10 W, λ = 1030 nm, τ = 250 fs, maximum repetition rate ν = 10 kHz) equipped with a PARUS optical parametric amplifier (Avesta-Project Ltd, Russia) was used, allowing to obtain laser radiation with wavelengths in the range of 400–800 nm. Using this laser system, the film surface was modified with the wavelengths λ = 400, 480, 550, 635 and 800 nm at a pulse duration of $\sim$150 fs. Laser radiation was focused at normal incidence onto the film using a microscope objective with a numerical aperture of NA = 0.03 into a spot with a diameter of 60 μm. A series of 300-μm-long scan lines were formed on the surface using each wavelength. The sample movement relative to the laser beam was implemented by three-axis motorized platform at a speed of 300 μm/s. The employed laser pulse repetition rates were ν = 1, 2, or 10 kHz and pulse energy E varied from 0.1 to 4.5 μJ. The laser pulse energy was measured using a 3A-P thermal power meter (Ophir, Israel), and the variation of the laser pulse energy was ensured by a continuous neutral density filter.

Visualization of the laser-irradiated sample surface for measuring the formed LIPSS periods was carried out using a scanning electron microscope (SEM, Vega 3, Tescan, Czech Republic), the measurement error for the periods was $\sim$5%. After that, to measure optical properties, square 400×400 μm^2 areas were written on the $As_{50}Se_{50}$ film surface, in the irradiation modes corresponding to the formation of LIPSS for each of the selected wavelengths. The optical transmission spectra of the areas with LIPSS were measured at room temperature using an MSFU-K microscope-spectrophotometer (LOMO, Russia); the measurements were carried out with an NA = 0.1 objective. Birefringence within the LIPSS-containing laser-irradiated areas was measured using a Thorlabs LCC7201B polarizing microscope (Thorlabs, USA) at 633 nm wavelength.

3. Results and discussion

Fig. 1 shows SEM images of HSFLs and LSFLs formed under laser irradiation with wavelengths of 400 and 480 nm. For both wavelengths, the formation of HSFLs and LSFLs is observed. The periods of the formed HSFLs were 120 and 180 nm, while those of the LSFLs were 370 and 455 nm, for the laser pulses wavelengths λ = 400 and 480 nm, respectively. Both types of structures were formed in the frequency range of 1–10 kHz, and for each frequency HSFL formation was observed at lower energies compared to LSFL.

With an increase in λ to 550 nm, HSFL with a period of 210 nm and LSFL with a period of 510 nm are formed (Fig. 2a,b). At this wavelength, LIPSS started to form at ν = 2 kHz and higher. At ν = 1 kHz, LIPSS were not observed up to energy of 0.88 μJ, when the film damage began (Fig. 2c). With irradiation at frequency of 2 kHz, HSFL formation was observed at the energy less than 0.38 μJ, and LSFL were observed in the energy range of 0.38–0.66 μJ. When irradiating with highest repetition rate of laser pulses (10 kHz), a hierarchical structure formation was observed, as can be seen in Fig. 2d, with simultaneous LSFL formation within the "grooves"-type LIPSS [10]. The period of the latter was about

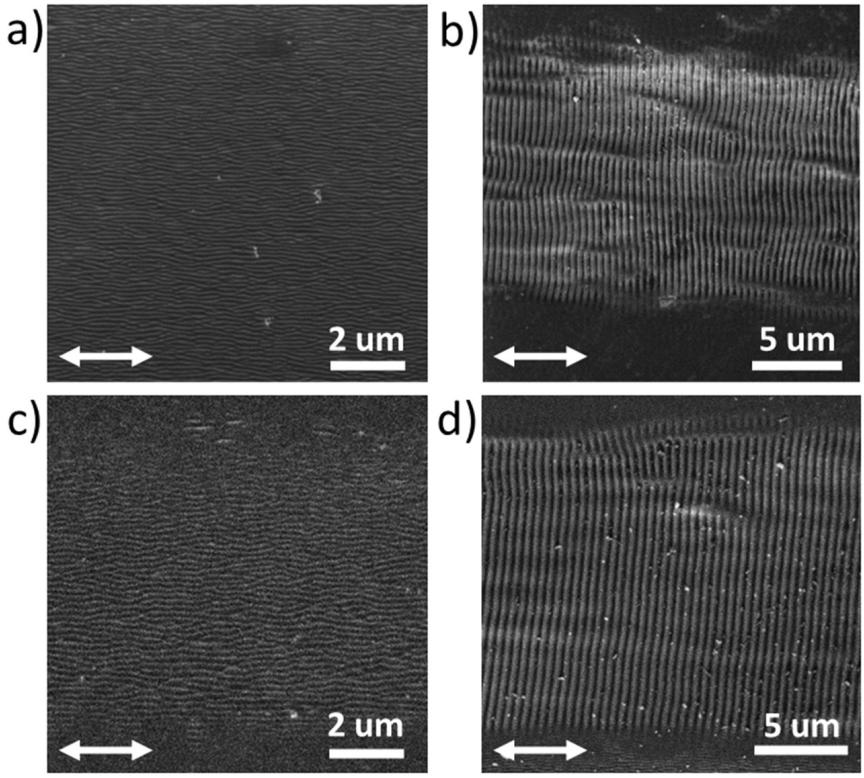

FIG. 1. SEM images of the LIPSS obtained at irradiation with femtosecond laser pulses at λ = 400 nm and (a) ν = 10 kHz, E = 0.14 μJ; (b) λ = 2 kHz, E = 0.6 μJ. LIPSS obtained at λ 480 nm and (c) ν = 10 kHz, E = 0.22 μJ; (d) ν = 2 kHz E = 0.51 μJ. Arrows indicate the laser polarization in each image

1.8 μm, which is higher than the laser wavelength, and the orientation was along the polarization vector of the laser radiation. No LSFL formation was detected at 10 kHz without the "grooves" for this wavelength.

At λ = 635 nm, the period of the surface relief was 230 nm for the HSFL, and 595 nm for the LSFL (Fig. 3a,b); both LIPSS types were formed in the range of ν from 2 to 10 kHz. Similar to the case with λ = 550 nm, at ν = 1 kHz, the LIPSS were not formed up to the laser pulse energy of 2.6 μJ, at which the film damage occurred. In this case, the film melted, forming ring-shaped structures containing fragmented LIPSS near the center of the scan line (Fig. 3d). And a complete film ablation was observed at the threshold laser pulse energy of 2.9 μJ. At a frequency of 2 kHz, LSFL began to form at the energy of 1.8 μJ (Fig. 3c), but their formation ceased with increasing energy. We also note that at ν = 10 kHz, similarly to λ = 550 nm, the formation of grooves was observed, with the period of $\sim$2.5 μm.

For λ = 800 nm, the formation of HSFLs began when using laser pulse energies of 3.1 and 1.8 μJ, at the repetition rates of 1 and 2 kHz, respectively. The period of the formed structures was 300 nm. However, with increasing energy, no LSFLs formation was observed at these repetition rates. Instead, periodic structures similar in appearance to HSFLs were formed in the central region of the scan line, parallel to the polarization of the laser pulses, but with a period of $\sim$720 nm, close to the LSFL period (Fig. 4a). When exceeding the laser pulse energies of 4.6 and 2.5 μJ for 1 and 2 kHz repetition rates respectively, the damage of the film was observed. Using ν = 10 kHz repetition rate, LSFLs were formed at the energy of 1.1 μJ. However, under these conditions, the film damage was observed in a few spots along the irradiated surface, which may be associated with a presence of initial defects in the film there. Contrary, at lower energies, the LIPSS were formed only near these defects. At laser pulse energies above 1.25 μJ and ν = 10 kHz, the film was damaged throughout the entire scanning area.

The dependence of the HSFL and LSFL periods on the laser wavelength is given in Fig. 5. The periods of the both LIPSS types increase linearly with the wavelength. In all cases, the LSFL period observed is slightly shorter than the laser wavelength, while the HSFL period is approximately 2.7 times shorter. The ratio of the LSFL to HSFL periods is about 2.5.

After determining the laser irradiation modes for the LIPSS formation for different wavelengths, 400$\times$400 μm^2 square areas were written to measure the birefringence of these structures. Since, HSFLs have weak birefringence properties due to low modulation of the relief [7], the modes in which LSFL formation occurs were used for each wavelength to obtain a higher birefringence value. Images of irradiated areas obtained by an optical polarizing microscope are shown in Fig. 6. The highest birefringence is observed for λ = 480 nm: corresponding retardance value, calculated as the difference in optical path length for ordinary and extraordinary waves, reaches 85 nm. For the LSFLs formed under irradiation with

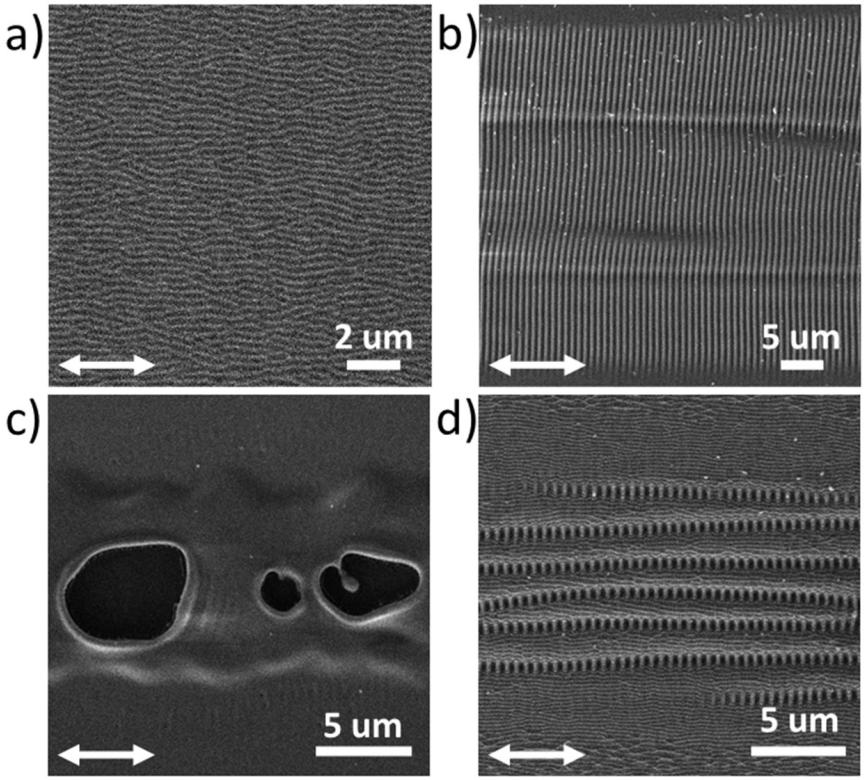

FIG. 2. SEM images of the surfaces irradiated with femtosecond laser pulses at λ = 550 nm and (a) ν = 2 kHz, E = 0.26 μJ; (b) ν = 2 kHz, E = 0.43 μJ; (c) ν = 1 kHz, E = 0.88 μJ; (d) ν = 10 kHz, E = 0.49 μJ. Arrows indicate the laser polarization in each image

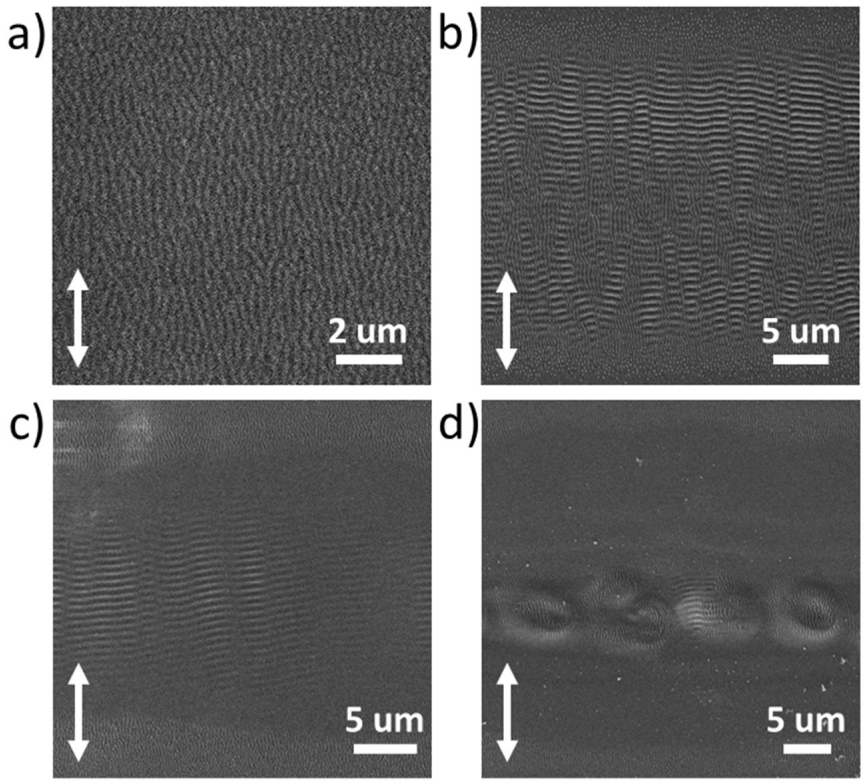

FIG. 3. SEM images of the surfaces irradiated with femtosecond laser pulses at λ = 635 nm and (a) ν = 2 kHz, E = 1.43 μJ; (b) ν = 10 kHz, E = 0.63 μJ; (c) ν = 2 kHz, E = 1.8 μJ; (d) ν = 1 kHz, E = 2.6 μJ. Arrows indicate the laser polarization in each image

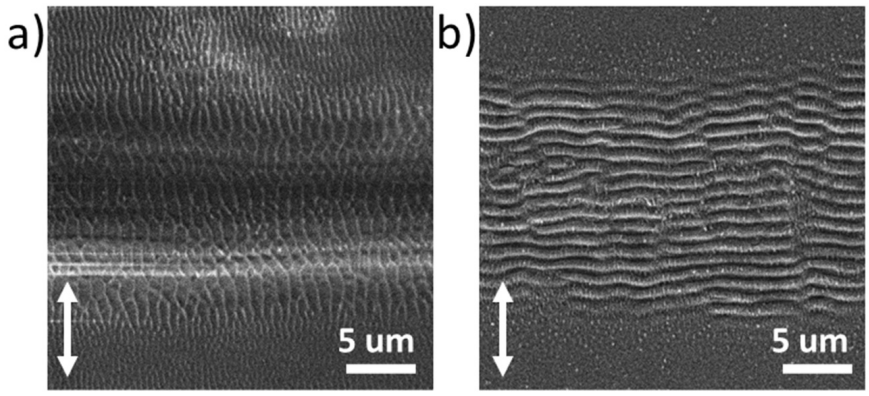

FIG. 4. SEM images of the LIPSS formed at $\lambda = 800$ nm and (a) $\nu = 1$ kHz, E = 4.0 μJ; (b) $\nu = 10$ kHz, E = 1.1 μJ. Arrows indicate the laser polarization in each image

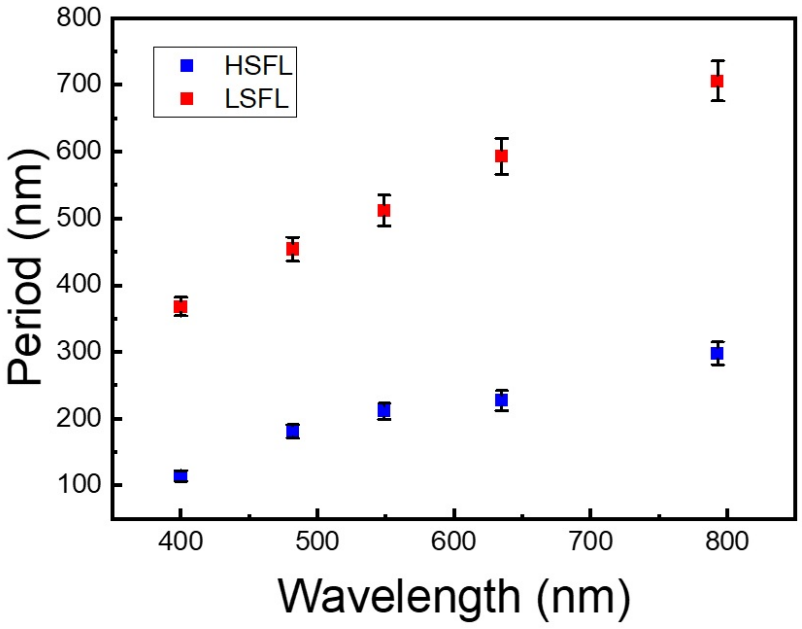

FIG. 5. The dependence of HSFL and LSFL periods on the laser radiation wavelength

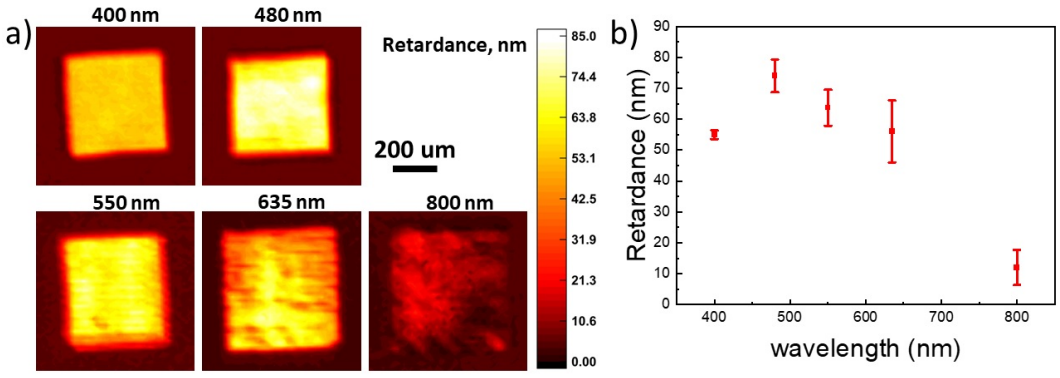

FIG. 6. Optical polarizing microscope images of LIPSS, formed at different wavelengths (a) and the dependence of the retardance on the laser writing wavelength (b)

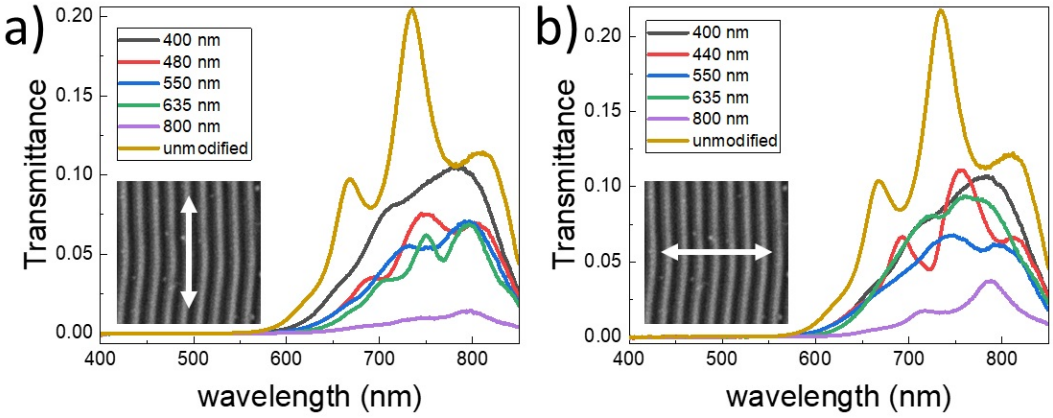

FIG. 7. Optical transmission spectra for the $As_{50}Se_{50}$ films with LIPSS in polarized light. The polarization of the transmitted light is (a) parallel or (b) orthogonal to the LIPSS ridges. The arrows indicate the polarization of the analyzed radiation relative to the LIPPS

λ = 400, 550 and 635 nm, the retardance values lie in the range of 50–75 nm. The minimum retardance value is observed for the LSFL formed at λ = 800 nm and does not exceed 20 nm. Thus, since the retardance value is related to the depth of the formed LIPSS [7, 14], the most prominent surface relief is formed at λ = 480 nm. Note that the photon energy for the laser radiation at λ = 635 nm has a value of $\sim$1.9 eV, exceeding the optical band gap of $As_{50}Se_{50}$, which is approximately 1.8 eV according to works [17, 18]. This ensures more efficient absorption of modifying laser light at this wavelength and the shorter ones as well, likely causing the formation of a more contrasting surface relief at laser irradiation with $\lambda \leq 635$ nm.

The presence of LIPSS also leads to a decrease in the optical transmission of the $As_{50}Se_{50}$ film. This is presumably due to the increased scattering by surface relief inhomogeneities formed as a result of laser irradiation. Fig. 7 presents the transmission spectra of LIPSS-containing regions on the $As_{50}Se_{50}$ film in polarized light. The spectra correspond to polarization of the transmitted radiation parallel (Fig. 7a) and orthogonal (Fig. 7b) to the ridges of the LIPSS. The structures formed with λ = 800 nm irradiation exhibit the greatest drop in transmission, which, combined with the lowest birefringence value, makes them of little interest for practical application. The smallest drop in transmission is observed for structures written at 400 nm, which may be due to their higher uniformity, compared to all other structures, as evidenced by the smallest variation in the retardance value within the irradiated area, observed in Fig. 6.

4. Conclusion

Examining formation of LIPSS on an $As_{50}Se_{50}$ films under femtosecond laser irradiation in this study allowed determining fabrication regimes for HSFLs and LSFLs at each wavelength used in the experiment from the 400–800 nm range. The LSFL structures formed at higher laser pulse energy compared to the HSFL. With increasing wavelength, a higher laser pulse repetition rate is also required to form LSFLs. Furthermore, specific formation regimes are discovered, for the LIPSS in a form of "grooves", as well as anomalous LSFL structures parallel to the laser polarization but with a period close to the laser wavelength. The dependence of LSFL birefringence on the wavelength of laser radiation used for the surface modification is determined in terms of optical retardance. The highest retardance up to 85 nm was observed for the region irradiated with laser pulses at a wavelength of 480 nm. For the LIPSS formed with $\lambda \leq$635 nm the retardance is at least 50 nm, while at longer wavelengths of the modifying laser radiation it drops to 12 nm. The formed LIPSSs reduce the transmittance of the ChGS film, which is most pronounced for structures written with irradiation at 800 nm.

References

[1] Iovu M.S., Shutov S.D., Popescu M. Relaxation of photodarkening in amorphous As–Se films doped with metals. *J. Non-Cryst. Solids*, 2002, **299**, P. 924–928.

[2] Arsh A., Klebanov M., Lyubin V., Shapiro L., Feigel A., Veinger M., Sfez B. Glassy $mAs_2S_3 \cdot nAs_2Se_3$ photoresist films for interference laser lithography. *Opt. Mater.*, 2004, **26**(3), P. 301–304.

[3] Flaxer E., Klebanov M., Abrahamoff D., Noah S., Lyubin V. Photodarkening of $As_{50}Se_{50}$ glassy films under μs light pulses. *Opt. Mater.*, 2009, **31**(4), P. 688–690.

[4] Savage J.A. Optical properties of chalcogenide glasses. *J. Non-Cryst. Solids*, 1982, **47**(1), P. 101–115.

[5] Petkov K., Ewen P.J.S. Photoinduced changes in the linear and non-linear optical properties of chalcogenide glasses. *J. Non-Cryst. Solids*, 1999, **249**(2), P. 150–159.

[6] Harbold J.M., Ilday F.Ö., Wise F.W., Sanghera J.S., Nguyen V.Q., Shaw L.B., Aggarwal I.D. Highly nonlinear As–S–Se glasses for all-optical switching. *Opt. Lett.*, 2002, **27**(2), P. 119–121.

[7] Shuleiko D., Zabotnov S., Sokolovskaya O., Poliakov M., Volkova L., Kunkel T., Kuzmin E., Danilov P., Kudryashov S., Pepelayev D., Kozyukhin S., Golovan L., Kashkarov P. Hierarchical Surface Structures and Large-Area Nanoscale Gratings in As_2S_3 and As_2Se_3 Films Irradiated with Femtosecond Laser Pulses. *Materials*, 2023, **16**(13), P. 4524.

[8] Yu X., Qi D., Wang H., Zhang Y., Wang L., Zhang Z., Dai Sh., Shen X., Zhang P., Xu Y. In situ and ex-situ physical scenario of the femtosecond laser-induced periodic surface structures. *Optics Express*, 2019, **27**(7), P. 10087–10097.

[9] Zabotnov S., Kolchin A., Shuleiko D., Presnov D., Kaminskaya T., Lazarenko P., Glukhenkaya V., Kunkel T., Kozyukhin S., Kashkarov P. Periodic relief fabrication and reversible phase transitions in amorphous $Ge_2Sb_2Te_5$ thin films upon multi-pulse femtosecond irradiation. *Micro*, 2022, **2**(1), P. 88–99.

[10] Bonse J., Kirner S.V., Krüger J. *Laser-Induced Periodic Surface Structures* (LIPSS). In: Sugioka, K. (eds) Handbook of Laser Micro- and Nano-Engineering. Springer, Cham, 2021, 59 p.

[11] Akhmanov S.A., Emel'yanov V.I., Koroteev N.I., Seminogov V.N. The effect of high-power laser radiation on the surface of semiconductors and metals: nonlinear optical effects and nonlinear optical diagnostics. *Sov. Phys. Usp.*, 1985, **147**(12), P. 675–745.

[12] Bonse J., Rosenfeld A., Krüger J. On the role of surface plasmon polaritons in the formation of laser-induced periodic surface structures upon irradiation of silicon by femtosecond-laser pulses. *Journal of Applied Physics*, 2009, **106**(10), P. 104910.

[13] Bonse J., Krüger J., Höhm S., Rosenfeld A. Femtosecond laser-induced periodic surface structures. *Journal of laser applications*, 2012, **24**(4), P. 042006.

[14] Kuzmin E., Zabotnov S., Shuleiko D., Pepelyaev D., Barbashov V., Efanov V., Kashkarov P. Laser-Induced Structuring of Arsenic Selenide Vitreous Films and Their Optical Properties. *Bulletin of the Russian Academy of Sciences: Physics*, 2024, **88**(3), P. S370–S374.

[15] Kozyukhin S., Lazarenko P., Vorobyov Yu., Baranchikov A., Glukhenkaya V., Smayev M., Sherchenkov A., Sybina Yu., Polohin A., Sigaev V. Laser-induced modification and formation of periodic surface structures (ripples) of amorphous GST225 phase change materials. *Optics and Laser Technology*, 2019, **113**, P. 87–94.

[16] Kozyukhin S., Smayev M., Sigaev V., Vorobyov Y., Zaytseva Y., Sherchenkov A., Lazarenko P. Specific features of formation of laser-induced periodic surface structures on $Ge_2Sb_2Te_5$ Amorphous Thin Films under Illumination by Femtosecond Laser Pulses. *Physica Status Solidi B*, 2020, **257**(11), P. 1900617.

[17] Corrales C., Ramírez-Malo J.B., Márquez E., Jiménez-Garay R. An optical study of the athermal photo-amorphization of $As_{50}Se_{50}$ thin films. *Materials Science and Engineering: B*, 1997, **47**(2), P. 119–126.

[18] Behera M., Naik P., Panda R., Naik R. Optical properties study in $As_{50}Se_{50}$ and $As_{50}Se_{40}Te_{10}$ chalcogenide thin films. Proceeding of "DAE SOLID STATE PHYSICS SYMPOSIUM 2016". Bhubaneswar, 2016, AIP Publishing LLC, 2017, P. 070009.

Submitted 16 November 2025; revised 23 November 2025; accepted 7 December 2025

Information about the authors:

Petr P. Pakholchuk – Lebedev Physical Institute, Russian Academy of Sciences, 53 Leninsky Avenue, Moscow 119991, Russia; Faculty of Physics, Moscow State University, 1/2 Leninskie Gory, Moscow, 119991, Russia; ORCID 0000-0002-2608-7621; p.paholchuk@lebedev.ru

Dmitrii V. Shuleiko – Faculty of Physics, Moscow State University, 1/2 Leninskie Gory, Moscow, 119991, Russia; ORCID 0000-0003-3555-6693; shuleyko.dmitriy@physics.msu.ru

Vadim A. Barbashov – Lebedev Physical Institute, Russian Academy of Sciences, 53 Leninsky Avenue, Moscow, 119991, Russia; ORCID 0000-0001-9615-3869; barbashovva@lebedev.ru

Stanislav V. Zabotnov – Faculty of Physics, Moscow State University, 1/2 Leninskie Gory, Moscow, 119991, Russia; ORCID 0000-0002-2528-4869; zabotnov@physics.msu.ru

Sergey A. Kozyukhin – Kurnakov Institute of General and Inorganic Chemistry, 31 Leninsky Avenue, Moscow, 119071, Russia; ORCID 0000-0002-7405-551X; sergkoz@igic.ras.ru

Pavel K. Kashkarov – Faculty of Physics, Moscow State University, 1/2 Leninskie Gory, Moscow, 119991, Russia; National Research Centre "Kurchatov Institute", 1 Akademika Kurchatova Sq., Moscow, 123182, Russia; ORCID 0000-0001-6889-001X; kashkarov@physics.msu.ru

Conflict of interest: the authors declare no conflict of interest.